2015

Epistasis Constrains Mutational Pathways of Hemoglobin Adaptation in High-Altitude Pikas

Danielle M. Tufts
University of Nebraska-Lincoln, dmtufts11@yahoo.com

Chandrasekhar Natarajan
University of Nebraska-Lincoln, chandrasekhar.natarajan@unl.edu

Inge G. Revsbech
Aarhus University, Denmark, inge.revsbech@biology.au.dk

Joana Projecto- Garcia
University of Nebraska, Lincoln

Federico G. Hoffmann
University of Nebraska - Lincoln, fhoffmann2@unl.edu

See next page for additional authors

Epistasis Constrains Mutational Pathways of Hemoglobin Adaptation in High-Altitude Pikas

Danielle M. Tufts,[†,1] Chandrasekhar Natarajan,[†,1] Inge G. Revsbech,[2] Joana Projecto-Garcia,[1] Federico G. Hoffmann,[3,4] Roy E. Weber,[2] Angela Fago,[2] Hideaki Moriyama,[1] and Jay F. Storz[*,1]

[1]School of Biological Sciences, University of Nebraska, Lincoln

[2]Department of Bioscience, Zoophysiology, Aarhus University, Aarhus, Denmark

[3]Department of Biochemistry, Molecular Biology, Entomology, and Plant Pathology, Mississippi State University

[4]Institute for Genomics, Biocomputing and Biotechnology, Mississippi State University

†These authors contributed equally to this work.

***Corresponding author:** E-mail: jstorz2@unl.edu.

Associate editor: David Irwin

Abstract

A fundamental question in evolutionary genetics concerns the roles of mutational pleiotropy and epistasis in shaping trajectories of protein evolution. This question can be addressed most directly by using site-directed mutagenesis to explore the mutational landscape of protein function in experimentally defined regions of sequence space. Here, we evaluate how pleiotropic trade-offs and epistatic interactions influence the accessibility of alternative mutational pathways during the adaptive evolution of hemoglobin (Hb) function in high-altitude pikas (Mammalia: Lagomorpha). By combining ancestral protein resurrection with a combinatorial protein-engineering approach, we examined the functional effects of sequential mutational steps in all possible pathways that produced an increased Hb–O_2 affinity. These experiments revealed that the effects of mutations on Hb–O_2 affinity are highly dependent on the temporal order in which they occur: Each of three β-chain substitutions produced a significant increase in Hb–O_2 affinity on the ancestral genetic background, but two of these substitutions produced opposite effects when they occurred as later steps in the pathway. The experiments revealed pervasive epistasis for Hb–O_2 affinity, but affinity-altering mutations produced no significant pleiotropic trade-offs. These results provide insights into the properties of adaptive substitutions in naturally evolved proteins and suggest that the accessibility of alternative mutational pathways may be more strongly constrained by sign epistasis for positively selected biochemical phenotypes than by antagonistic pleiotropy.

Key words: **adaptation, epistasis, hemoglobin, high altitude, molecular evolution, protein evolution.**

Introduction

The adaptive evolution of protein function may typically involve the sequential fixation of individual amino acid mutations with each substitution producing an incremental improvement in the selected biochemical phenotype. However, there are two interrelated factors that can potentially affect fixation probabilities and constrain the number of selectively accessible pathways to high-fitness genotypes: Mutational pleiotropy (where a given mutation perturbs multiple phenotypes) and epistasis (nonadditive interactions between mutations). As amino acid mutations often affect multiple aspects of protein biochemistry (Taverna and Goldstein 2002; Wang et al. 2002; DePristo et al. 2005; Bloom et al. 2006; Weinreich et al. 2006; Tokuriki et al. 2008; Tokuriki and Tawfik 2009), mutations that improve one aspect of protein function may simultaneously compromise other functions. Pleiotropic trade-offs can also give rise to a context-dependence of mutational effects, as the phenotypic effect of a given mutation may be contingent on the existence of compensatory mutations at other sites in the same protein.

During the adaptive evolution of a particular protein function, epistasis can affect the fixation probabilities of function-altering mutations and influence trajectories of protein evolution in two ways: 1) The sign or magnitude of the mutation's effect on the selected phenotype may be conditional on genetic background, and 2) the sign or magnitude of the mutation's pleiotropic effects may be conditional on genetic background. Both forms of epistatic interaction can influence whether evolution is more likely to follow some pathways rather than others (Weinreich et al. 2006; DePristo et al. 2007; Ortlund et al. 2007; Poelwijk et al. 2007; Bridgham et al. 2009; Lozovsky et al. 2009; Carneiro and Hartl 2010; da Silva et al. 2010; Kryazhimskiy et al. 2011, 2014; Kvitek and Sherlock 2011; Rokyta et al. 2011; Salverda et al. 2011; Ostman et al. 2012; Weinreich and Knies 2013; de Visser and Krug 2014; Harms and Thornton 2014).

A compelling system for investigating the pleiotropic and epistatic effects of function-altering mutations is provided by the evolution of increased hemoglobin (Hb)-O_2 affinities in vertebrate species that have adapted to environmental hypoxia. Among vertebrates, elevated Hb–O_2 affinities have

evolved in multiple species that have adapted to chronic O_2 deprivation at high altitude (Storz 2007; Weber 2007; Storz and Moriyama 2008; Storz et al. 2009; Storz, Runck et al. 2010; Natarajan et al. 2013; Projecto-Garcia et al. 2013; Revsbech et al. 2013). Under severe hypoxia, an increased Hb–O_2 affinity can help preserve an adequate level of tissue oxygenation by enhancing pulmonary O_2 uptake while simultaneously maintaining the pressure gradient that drives O_2 diffusion from capillary blood to the tissue mitochondria (reviewed by Storz, Scott et al. 2010; Mairbäurl and Weber 2012). Even slight increases in Hb–O_2 affinity can efficiently safeguard arterial O_2 saturation under hypoxia, thereby complementing numerous other physiological adjustments in the cardiopulmonary system (Turek and Kreuzer 1976; Turek, Kreuzer, Ringnalda 1978; Turek, Kreuzer, Turek-Maischeider, et al. 1978; Mairbäurl 1994).

Mammalian Hb is a heterotetramer, consisting of two α-type subunits and two β-type subunits that each contain a heme group—a porphyrin ring with a ferrous (Fe^{2+}) iron atom capable of reversibly binding a single dioxygen molecule. The Hb tetramer undergoes an oxygenation-linked transition in quaternary structure, whereby the two semirigid $\alpha_1\beta_1$ and $\alpha_2\beta_2$ dimers rotate around each other by 15° during the transition between the deoxy (T-state) and oxy (R-state) conformations (Perutz 1972, 1989; Baldwin and Chothia 1979). This oxygenation-linked shift in quaternary structure between the T- and R-states is central to the allosteric function of Hb as an O_2-transport molecule, and underpins the subunit cooperativity of O_2-binding as well as the sensitivity of O_2-affinity to allosteric effectors such as protons, Cl- ions, and organic phosphates. Allosteric effectors have the effect of reducing Hb–O_2 affinity because they preferentially bind to deoxyHb, thereby stabilizing the low-affinity T structure through the formation of additional hydrogen-bonds and salt bridges within and between subunits (Bettati et al. 1983; Perutz 1989).

There are numerous possible mutational changes that can alter Hb–O_2 affinity, but many or most such changes have deleterious pleiotropic effects on other structural or functional properties (Bellelli et al. 2006; Bonaventura et al. 2013; Varnado et al. 2013). For example, active site mutations that alter the polarity or hydrophobicity of the distal heme pocket can produce significant changes in ligand affinity, but such mutations can reduce structural stability and/or increase rates of spontaneous heme oxidation (autoxidation), which renders the oxidized Fe^{3+} "metHb" incapable of O_2-binding (Varnado et al. 2013). Similarly, mutations that increase Hb–O_2 affinity by suppressing sensitivity to allosteric effectors sacrifice an important mechanism of phenotypic plasticity because changes in intraerythrocytic concentrations of organic phosphates and other effectors are rendered less effective as a means of modulating blood–O_2 affinity in response to transient changes in metabolic demand or environmental O_2 availability. Thus, mutations with identical main effects on Hb–O_2 affinity may still be unequal in the eyes of natural selection if they vary in the magnitude of antagonistic pleiotropy (Otto 2004; Streisfeld and Rausher 2011).

To assess the roles of pleiotropy and epistasis in the evolution of protein function, we used a combinatorial protein engineering approach to dissect the mechanistic basis of evolved differences in Hb–O_2 affinity between two sister species of North American pikas (Mammalia: Lagomorpha) that have contrasting altitudinal range limits. Our comparison included the American pika (*Ochotona princeps*), an alpine specialist, and the closely related collared pika (*O. collaris*), which has a predominantly lowland distribution in Alaska and northwestern Canada. *Ochotona princeps* inhabits the highest summits in the contiguous United States at elevations of approximately 4,300 m where the partial pressure of O_2 (PO_2) is 60% of the sea level value (~96 vs. ~160 torr). Pikas originated and diversified in the Palearctic (Erbajeva 1994), and *O. princeps* and *O. collaris* represent the only two extant pika species in North America. The two species diverged approximately 4–8 Ma (Lanier and Olson 2009). Although *O. princeps* is mainly found above timberline in high-altitude talus habitats (Smith and Weston 1990; Hafner 1994), fossils and biogeographic evidence indicate that the species also inhabited lower elevations during Quaternary glacial cycles (Mead 1987; Hafner 1993; Galbreath et al. 2009, 2010; Lanier and Olson 2013). Because of the dramatic difference in elevational range limits between *O. princeps* and *O. collaris*, comparisons between these two closely related species provide an opportunity to identify the molecular basis of evolved differences in Hb function that may have adaptive significance.

Using ancestral protein resurrection and site-directed mutagenesis, we measured the structural and functional effects of sequential mutations in all possible pathways connecting the resurrected ancestral (low-affinity) Hb and the derived (high-affinity) Hb of the high-altitude species. In addition to measuring oxygenation properties of each engineered recombinant Hb (rHb) mutant, we also measured pleiotropic effects on functional properties that can potentially trade-off with Hb–O_2 affinity.

The experiments were designed to answer the following questions: 1) What fraction of the evolved change in Hb–O_2 affinity is attributable to substitutions at each step in the pathway? 2) Are the functional effects of mutations conditional on genetic background? For example, do the functional effects of individual mutations depend on the sequential order in which they occur? And 3) Do affinity-enhancing mutations have deleterious pleiotropic effects on other structural or functional properties? The experimental results revealed that the sign and magnitude of mutational effects on Hb–O_2 affinity were highly dependent on the genetic background in which they occurred, but affinity-altering mutations produced no significant pleiotropic effects on other aspects of Hb function.

Results and Discussion

For the experimental analysis of Hb function, we collected specimens of *O. princeps* from a high-altitude locality in the Southern Rockies and specimens of *O. collaris* from lowland localities in interior Alaska (see Materials and Methods). We experimentally confirmed that both species express a single tetrameric $\alpha_2\beta_2$ Hb isoform during adult life, consistent with

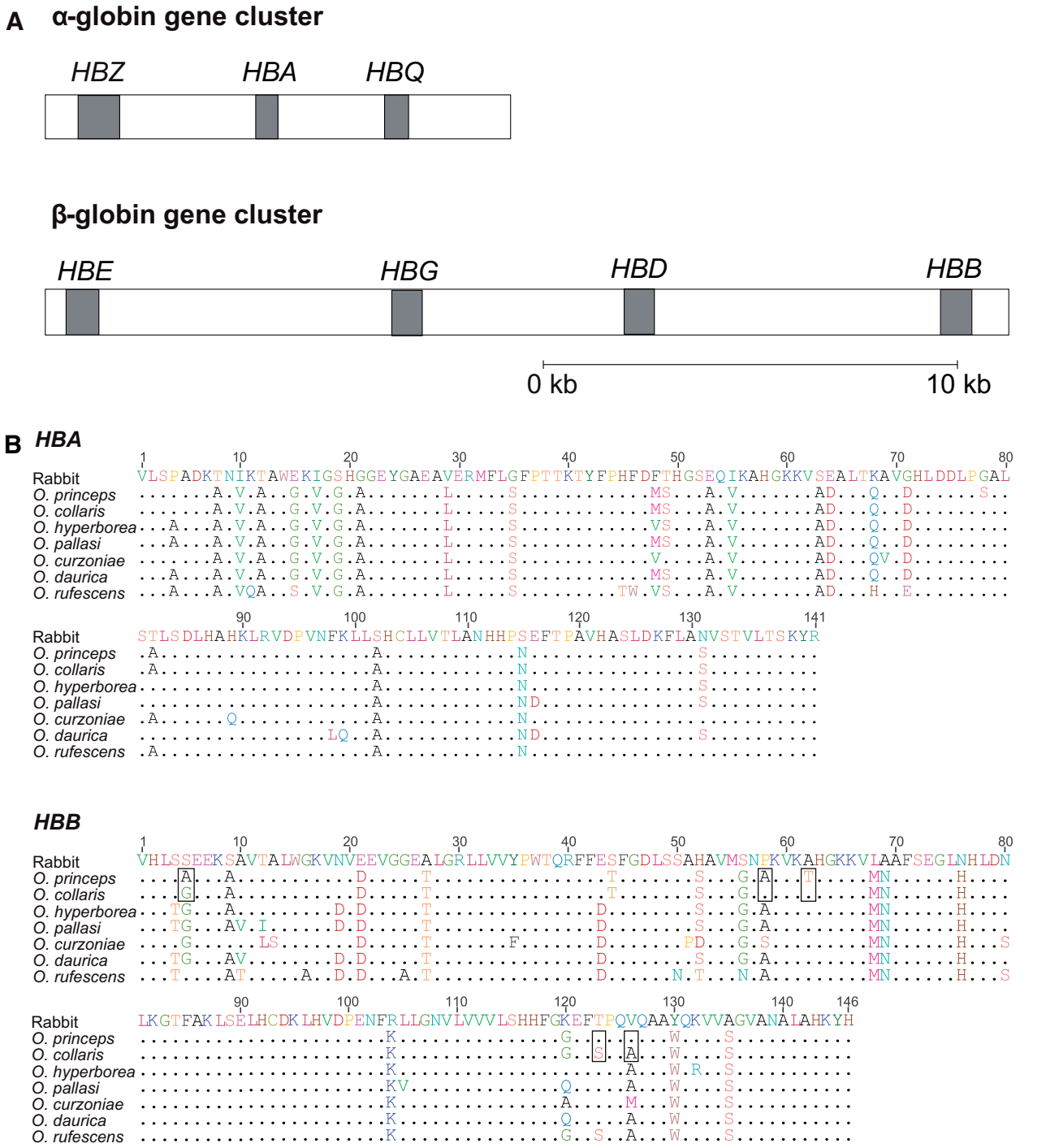

Fig. 1. Pika globin genes. (*A*) Genomic structure of the α- and β-globin gene clusters of *Ochotona princeps* (GenBank accession numbers NT_167265 and AC234505, respectively). Isoelectric focusing experiments revealed that adult *O. princeps* and *O. collaris* both express a single, tetrameric $\alpha_2\beta_2$ Hb isoform that incorporates the α-chain products of the *HBA* gene, and β-chain products of the *HBB* gene. Products of the remaining α- and β-like globin genes are not incorporated into functional Hb tetramers in definitive erythrocytes. Based on data from other eutherian mammals, products of three of the remaining globin genes are expected to encode α-type (*HBZ* [ζ-globin]) or β-type (*HBE* [ε-globin] and *HBG* [γ-globin]) subunits that are incorporated into structurally distinct Hb isoforms that are expressed at different stages of prenatal development. (*B*) Alignment of HBA and HBB amino acid sequences from seven pika species, including the two North American sister species, *O. princeps* and *O. collaris*. Orthologous sequences from the European rabbit (*Oryctolagus cuniculus*) are provided for comparison. In addition to the five β-chain substitutions at sites 5, 58, 62, 123, and 126 that distinguish the Hbs of *O. princeps* and *O. collaris* (denoted by boxes), there is one nearly fixed difference at site 78 in the α-chain.

genomic evidence that *O. princeps* possesses single copies of postnatally expressed α- and β-globin genes (*HBA* and *HBB*, respectively; fig. 1*A*). We sequenced both *HBA* alleles and both *HBB* alleles from multiple individuals per species. The sequence data revealed that the Hbs of the two species are distinguished by five amino acid substitutions in the β-chain subunits (sites β5, β58, β62, β123, and β126; fig. 1*B*). Using blood samples from individuals with known

HBA and *HBB* genotypes, we tested for differences in the oxygenation properties of purified Hbs from highland *O. princeps* ($n = 4$) and lowland *O. collaris* ($n = 4$) that were distinguished by the five β-chain substitutions. To gain insights into functional mechanisms that may be responsible for evolved differences in O_2-binding properties, we measured O_2-affinities of purified Hbs under four treatments: In the absence of allosteric effectors (stripped), in the presence of Cl^- ions (added as 0.1 M KCl), in the presence of 2,3-diphosphoglycerate (DPG, at 2-fold molar excess over tetrameric Hb), and in the simultaneous presence of KCl and DPG. The (KCl+DPG) treatment most closely approximates in vivo conditions in mammalian red blood cells (Mairbäurl and Weber 2012), so from this point forward we focus on comparisons of Hb–O_2 affinity in the presence of anionic effectors.

The experiments revealed that the Hb of *O. princeps* exhibits a uniformly higher O_2-affinity than that of *O. collaris*, as indicated by the lower values of P_{50} (the partial pressure of O_2 at which Hb is 50% saturated; table 1 and fig. 2*A*). The Hb of *O. princeps* exhibited a significantly higher intrinsic O_2 affinity than that of *O. collaris*, as indicated by the lower P_{50} for stripped Hb ($P_{50(\text{stripped})}$), and this difference persisted in the presence of Cl^- ions ($P_{50(\text{KCl})}$), in the presence of DPG ($P_{50(\text{DPG})}$), and in the simultaneous presence of both allosteric effectors ($P_{50(\text{KCl+DPG})}$; table 1 and fig. 2*A*). Measures of allosteric regulatory capacity (fig. 2*B*) revealed that the species differences in $P_{50(\text{KCl+DPG})}$ were exclusively attributable to differences in intrinsic O_2 affinity; there were no appreciable differences in the responsiveness to allosteric effectors. This was confirmed by dose–response curves for DPG, which demonstrated that Hb–O_2 affinities of both species had identical association constants for DPG binding (fig. 3). Hbs of both species were also characterized by highly similar cooperativity coefficients (table 1).

Table 1. O_2-Affinities (P_{50}, torr) and Cooperativity Coefficients (n_{50}) (mean ± SEM) of Purified Hbs from High- and Low-Altitude Pika Species (*Ochotona princeps* and *O. collaris*, respectively).

	O. princeps (high altitude) ($n = 4$)	*O. collaris* (low altitude) ($n = 4$)
P_{50} (torr)		
Stripped	**5.20 ± 0.29**	**6.23 ± 0.16**
+KCl	**10.07 ± 0.65**	**11.66 ± 1.32**
+DPG	**10.51 ± 0.63**	**12.91 ± 0.31**
KCl + DPG	**11.24 ± 0.69**	**13.24 ± 0.33**
n_{50}		
Stripped	**1.99 ± 0.21**	**2.35 ± 0.05**
+KCl	**2.53 ± 0.20**	**2.54 ± 0.06**
+DPG	**2.41 ± 0.09**	**2.56 ± 0.22**
KCl + DPG	**2.51 ± 0.16**	**2.58 ± 0.05**

NOTE.—O_2-equilibrium curves were measured at 0.3 mM heme in 0.1 M HEPES buffer at pH 7.4, 37 °C, in the absence (stripped) and presence of added KCl (0.1 M) and/or DPG (DPG/Hb tetramer ratio, 2.0), as indicated. Sample sizes refer to the number of individuals analyzed per species.

Sequence data from additional species of pikas enabled us to reconstruct the β-chain sequence of the *princeps*/*collaris* common ancestor (Anc1; fig. 4*A*). For each of the five amino acid sites, posterior probabilities of estimated ancestral states were as follows: β5G (1.000), β58A (0.984), β62A (0.987), β123T (0.997), and β126A (0.947). The ancestral sequence reconstruction revealed that three of the five β-chain substitutions that distinguish the Hbs of the two species occurred on the branch leading to the high-altitude *O. princeps*, β5Gly→Ala (βG5A), β62Ala→Thr (βA62T), and β126Ala→Val (βA126V), and the remaining two substitutions occurred on the branch leading to the low-altitude *O. collaris*, β58Ala→Pro (βA58P) and β123Thr→Ser (βT123S) (fig. 4*A*). As a first step in the protein-engineering experiments, we synthesized, purified, and functionally tested rHbs representing the wildtype Hbs of *O. princeps* and *O. collaris* and the reconstructed Hb of their common ancestor, Anc1 (fig. 4*A*). A triangulated comparison involving the reconstructed Anc1 and its modern-day descendants revealed that the elevated Hb–O_2 affinity of *O. princeps* is a derived character state: $P_{50(\text{KCl+DPG})}$ for the highland *O. princeps* rHb was 21.8% lower (i.e., O_2 affinity was higher) relative to Anc1 (supplementary table S1, Supplementary Material

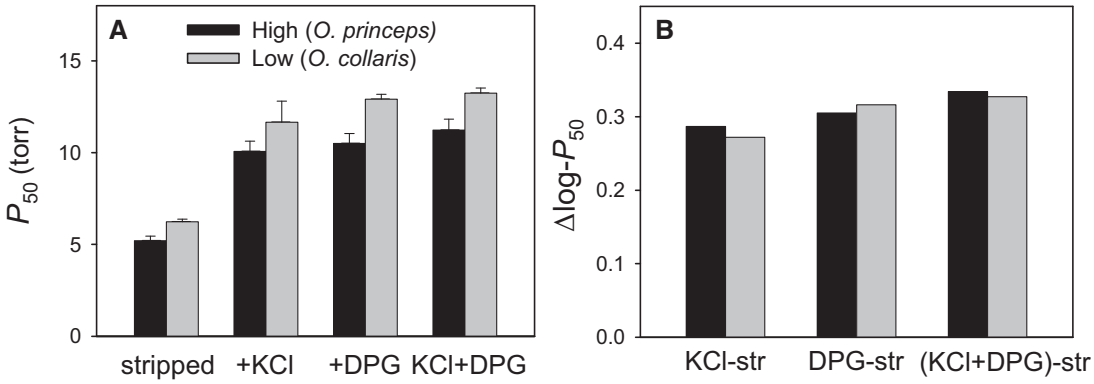

FIG. 2. Hbs of the high-altitude *Ochotona princeps* exhibit uniformly higher O_2-affinities than those of the low-altitude *O. collaris*. (*A*) P_{50} values (mean ± SEM) for purified Hbs of *O. princeps* ($n = 4$ individuals) and *O. collaris* ($n = 4$ individuals), measured at pH 7.4 and 37 °C in the absence (stripped) and presence of allosteric effectors ([Cl^-], 0.1 *M*; [HEPES], 0.1 *M*; DPG/Hb tetramer ratio, 2.0; [heme], 0.3 mM). (*B*) Log-transformed differences in P_{50} values of Hbs from *O. princeps* and *O. collaris* in the presence and absence of allosteric effectors. The $\Delta\log\text{-}P_{50}$ values measure the extent to which Hb–O_2 affinity is reduced in the presence of a given allosteric effector (Cl^-, DPG, or both anions together). See table 1 for raw data.

online). Consistent with our experiments on the native Hbs, $P_{50(KCl+DPG)}$ for the highland *O. princeps* rHb was 14.4% lower relative to the lowland *O. collaris* rHb. In conjunction with the ancestral sequence reconstruction, these results indicate that the derived increase in O_2 affinity of *O. princeps* Hb was attributable to the independent or joint effects of the three substitutions at sites β5, β62, and β126 (fig. 4*A*).

To complement experimental measures of the functional effects of each amino acid substitution, we used a codon-based maximum-likelihood approach to test for evidence of positive selection in an alignment of *HBA* and *HBB* sequences from all examined pika species (see Materials and Methods).

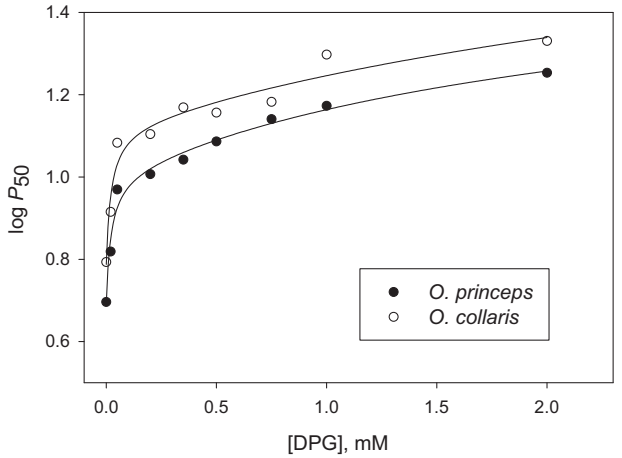

Fig. 3. Variation in Hb–O_2 affinity (as indexed by P_{50}) as a function of DPG concentration for purified Hbs of *Ochotona princeps* and *O. collaris*. Curves were fit using a double hyperbolic function. The Hbs of the two pika species exhibit no discernible difference in DPG binding constants, with an apparent dissociation equilibrium constant for the high-affinity DPG site of approximately 0.02 mM.

In the case of *HBB*, likelihood ratio tests (LRTs) revealed significant variation among sites in the ratio of nonsynonymous-to-synonymous substitution rates ($\omega = d_N/d_S$), and a branch-sites test (Zhang et al. 2005; Yang and dos Reis 2011) implicated positive selection in driving substitutions at both β62 and β126 in *O. princeps* (supplementary table S2, Supplementary Material online).

We used site-directed mutagenesis to synthesize the inferred ancestral genotype (Anc1), the derived, triple-mutant genotype of *O. princeps*, and each of the six possible mutational intermediates that connect them (fig. 4*B*). This combinatorially complete set of three-site genotypes enabled us to measure the additive and nonadditive effects of *princeps*-specific substitutions on each of eight (= 2^3) possible genetic backgrounds. Of the six (=3!) possible forward trajectories that lead from Anc1 to the derived, triple-mutant β-globin genotype of *O. princeps*, our experiments revealed that only a single pathway yielded an incremental increase in Hb–O_2 affinity at each successive step: βG5A (first), βA62T (second), and βA126V (third; fig. 5). Each of the three possible first mutational steps produced a significant increase in Hb–O_2 affinity, as did one of six possible second steps (A126V on the "AAA" background) and one of three possible final steps (βA126V on the "ATA" background; fig. 5). However, each mutation's effect on Hb–O_2 affinity was highly dependent on the genetic background in which it occurred, as one of six possible second steps (βG5A) and two of three possible final steps (βG5A and βA62T) yielded significant "reductions" in Hb–O_2 affinity. The βG5A and βA62T substitutions exhibited sign epistasis for Hb–O_2 affinity: Both substitutions significantly increased affinity on the Anc1 background, but they both produced opposite effects when they occurred on backgrounds in which the other substitutions had already occurred (fig. 5; supplementary table S1, Supplementary

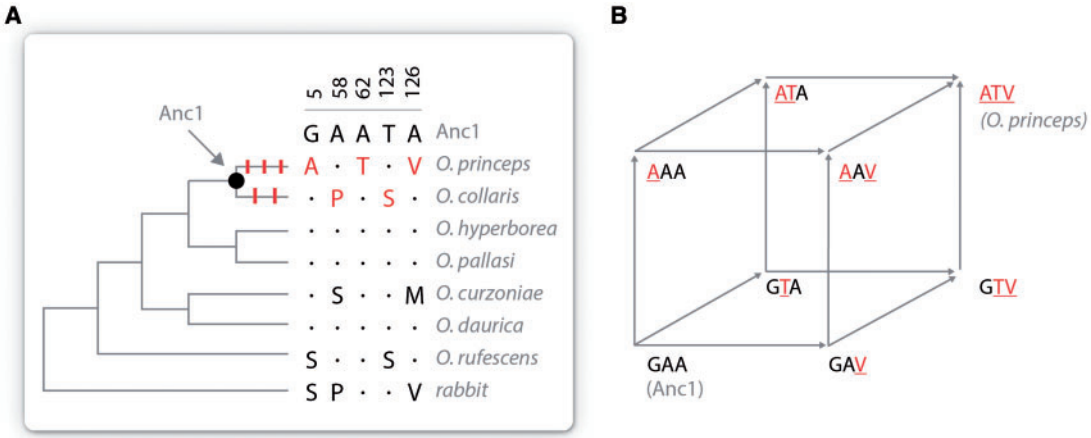

Fig. 4. Inferred history of substitution at five sites that distinguish the *HBB* genes of the high-altitude *Ochotona princeps* and the low-altitude *O. collaris*. (*A*) Of the five amino acid substitutions that distinguish the Hbs of the two sister species, ancestral sequence reconstruction revealed that three occurred on the branch leading to *O. princeps*, and the remaining two occurred on the branch leading to *O. collaris*. "Anc1" represents the reconstructed HBB sequence of the *princeps*/*collaris* common ancestor. The phylogeny of pika species is taken from (Lanier and Olson 2009). (*B*) Graphical representation of sequence space, where each vertex of the cube represents a discrete three-site β5–β62–β126 genotype and each edge connects genotypes separated by a single mutational step. The low-affinity ancestral Anc1 and the high-affinity Hb of *O. princeps* are connected by six (=3!) possible forward trajectories through sequence space.

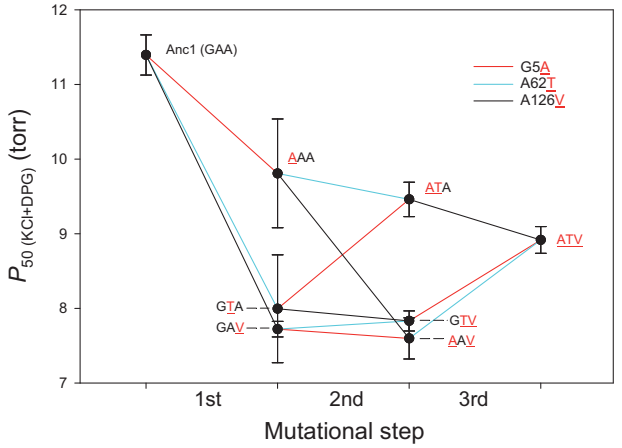

Fig. 5. Trajectories of change in Hb–O_2 affinity (indexed by $P_{50(KCl+DPG)}$) for each of six forward mutational pathways leading from the ancestral three-site $\beta5$–$\beta62$–$\beta126$ "Anc1" genotype (GAA) to the derived, triple-mutant genotype of *O. princeps* (ATV). Only one of six possible forward pathways yields a monotonic increase in Hb–O_2 affinity: G5A (1st), A62T (2nd), A126V (3rd). Error bars denote 95% confidence intervals.

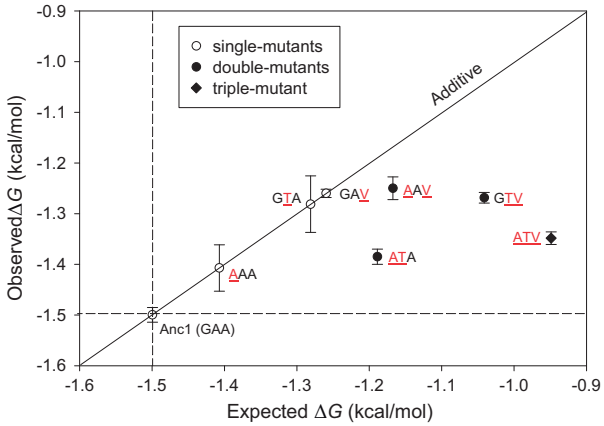

Fig. 6. Relative to the ancestral genotype (Anc1), pairwise epistasis for the free energy of Hb–O_2 binding, ΔG, was consistently negative (indicating negative epistasis for Hb–O_2 affinity). ΔG values for the double- and triple mutant genotypes were measured relative to Anc1 and were plotted against values expected under an additive model. Observed ΔG's for the full set of double- and triple-mutant genotypes fell below the $y = x$ diagonal, reflecting the fact that the combined effects of affinity-altering mutations were consistently less than the sum of their individual effects on the Anc1 background. Error bars denote 95% confidence intervals.

Material online). Similar sign-epistatic effects of affinity-altering mutations have been documented in protein engineering studies of other vertebrate Hbs (Natarajan et al. 2013; Projecto-Garcia et al. 2013).

In contrast to the sign-epistatic effects of βG5A and βA62T, the βA126V substitution had an affinity-enhancing effect on each of the four possible genetic backgrounds (fig. 5), although the magnitude of the affinity-enhancing effect was highly context-dependent: βA126V produced a 32.2% reduction in $P_{50(KCl+DPG)}$ when it occurred as the first substitution (on the Anc1 background) compared with a 5.8% reduction when it occurred as the final substitution (on a background in which βG5A and βA62T had already occurred). Relative to the Anc1 reference genotype, pairwise epistasis was consistently negative for the free energy of Hb–O_2 binding (ΔG), indicating that the combined effects of affinity-altering mutations were always less than the sum of their individual effects on the Anc1 background (fig. 6).

Structural Basis of Mutational Effects

Homology modeling and comparative data from human Hb mutants provided insights into the structural mechanisms responsible for the individual functional effects of *HBB* substitutions in the *O. princeps* lineage. The βG5A substitution is predicted to stabilize the A-helix of the β-chain by reducing backbone entropy and by reducing the solvent accessibility of apolar surface (Lopez-Llano et al. 2006). This stabilization of α-helical conformation can propagate to the $\alpha_1\beta_2$ and $\alpha_2\beta_1$ intersubunit contacts that mediate oxygenation-linked transitions in quaternary structure, thereby perturbing the allosteric equilibrium between the high-affinity (R-state) and low-affinity (T-state) conformations (Dumoulin et al. 1997, 1998; Bellelli et al. 2006).

The βA62T substitution is predicted to increase the rigidity of the E-helix because the γ-oxygen atom of β62Thr forms a polar contact with the β58Ala main-chain oxygen atom (fig. 7). This localized stabilization of E-helix secondary structure produces a subtle conformational change in the β-chain distal heme pocket, thereby reducing steric hindrance of β heme ligand-binding. Similarly, a nonpolar→polar βA62P mutation at the same site in human Hb (Hb Duarte) also produces an increased O_2 affinity while preserving normal cooperativity and DPG sensitivity (Beutler et al. 1974; Ceccarelli et al. 2006). The structural mechanisms responsible for the observed interaction effects are not immediately clear, as sites $\beta5$, $\beta62$, and $\beta126$ are structurally remote from one another in the folded β-chain subunit (fig. 7), indicating that epistatic interactions do not involve direct steric contact between residue side chains or short-range steric interaction mediated by a third residue or bound ligand. Instead, the observed epistatic effects must stem from indirect, second-order perturbations, possibly involving dynamics of the allosteric transition in quaternary structure between different oxygenation states of the Hb tetramer.

Pleiotropic Trade-Offs

Analysis of the full set of rHb mutants revealed that Hb–O_2 affinity in the presence of allosteric effectors ($P_{50(KCl+DPG)}$) was not significantly correlated with allosteric regulatory capacity, as measured by both Cl^- sensitivity ($r = -0.263$, $P = 0.530$) and DPG sensitivity ($r = -0.200$, $P = 0.636$), the cooperativity of O_2-binding, as measured by Hill's cooperativity coefficient, n_{50} ($r = 0.313$, $P = 0.450$), autoxidation rate ($r = 0.066$, $P = 0.877$), or structural mobility, as measured by a computationally predicted index of energetic frustration (Jenik et al. 2012) ($r = -0.451$, $P = 0.262$). Functional experiments on the engineered rHb mutants revealed sign and magnitude epistasis for Hb–O_2 affinity, but affinity-altering mutations

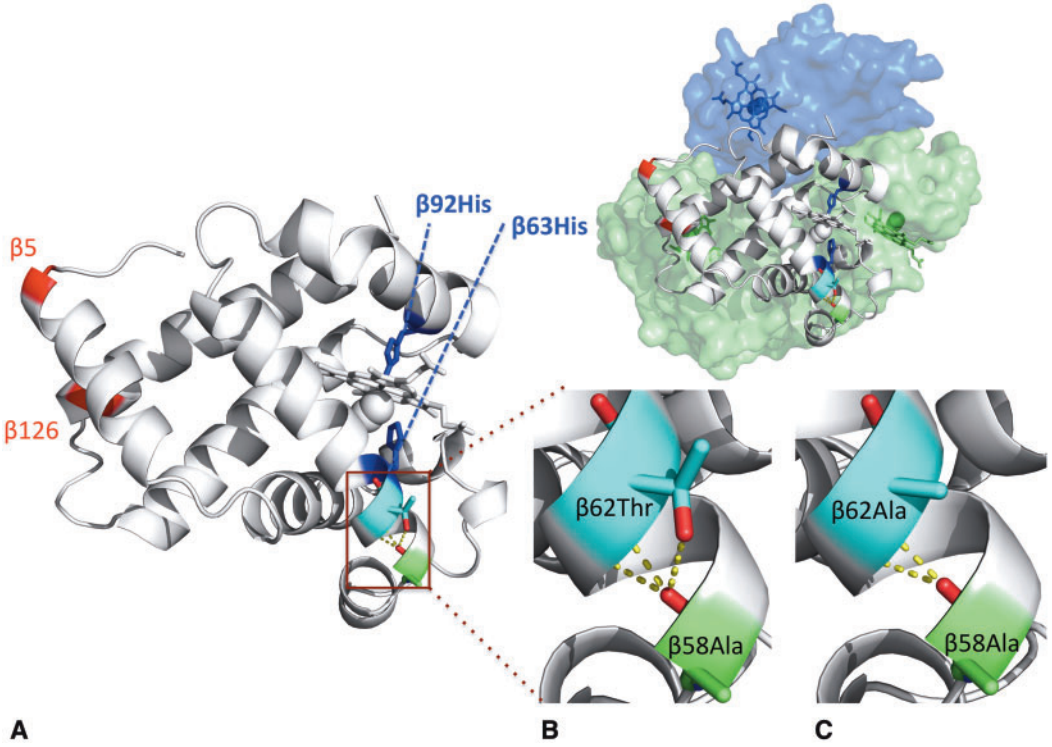

Fig. 7. Homology model of pika Hb showing detailed view of the β1 subunit, and the locations of three amino acid substitutions (βG5A, βA62T, and βA126V) that occurred in the *Ochotona princeps* lineage (*A*). The proximal histidine, β92 (which covalently binds the fifth coordination site of the heme iron), and the distal histidine, β63 (which stabilizes bound ligand at the sixth coordination site on the opposite side of the heme plane), are shown in blue. Counting from the N-terminal valine of the β-chain polypeptide, β5 is the second residue of the A helix, β62 is the sixth residue of the E-helix, and β126 is the fourth residue of the H helix. Inset (top right) shows the full Hb tetramer, with the focal β1 subunit depicted as a ribbon structure; the β2 subunit is shown in blue, and the α1 and α2 subunits are shown in green. (*B*) The βA62T substitution increases the rigidity of the E-helix because the γ-oxygen atom of β62Thr forms a polar contact with the β58Ala main-chain oxygen atom. (*C*) The methyl side-chain of the ancestral β62Ala forms no contact with β58Ala, resulting in a less stable α-helical conformation.

produced no appreciable effects on other structural or functional properties that potentially trade-off with O_2-affinity.

The substitutions that we examined are substitutions that actually occurred in the ancestry of modern-day *O. princeps*. It may be that the pleiotropic and epistatic effects of substitutions that actually did occur are qualitatively or quantitatively distinct from those of all possible affinity-altering substitutions that could have occurred (Draghi and Plotkin 2013; Gong and Bloom 2014). More general conclusions about how pleiotropy influences the fixation probabilities of mutations can be obtained by comparing the spectrum of substitutions that have actually contributed to evolutionary changes in protein function with the spectrum of spontaneous mutations that affect protein function (Streisfeld and Rausher 2011).

Evolutionary Implications of Sign Epistasis between Affinity-Altering Mutations

Insights into the form and prevalence of intramolecular epistasis can illuminate the extent to which realized pathways of protein evolution represent deterministic or historically contingent outcomes. Epistasis between mutant sites in the same protein can exert a deterministic influence on molecular evolution by constraining the number of selectively accessible mutational pathways to high-fitness genotypes, thereby enhancing the repeatability (and hence, predictability) of adaptive walks through sequence space (Weinreich et al. 2005, 2006; DePristo et al. 2007; Lozovsky et al. 2009; da Silva et al. 2010; Rokyta et al. 2011). However, epistasis can also exert a stochastic influence because if the phenotypic effects of mutations are conditional on the genetic background in which they occur, then the range of selectively accessible mutational pathways will be historically contingent on which particular mutations happen to occur first (Kvitek and Sherlock 2011; Salverda et al. 2011; Harms and Thornton 2014; Kryazhimskiy et al. 2014).

If the derived increase in Hb–O_2 affinity in the *O. princeps* lineage evolved under the influence of positive directional selection (as suggested by results of the branch-sites test; supplementary table S2, Supplementary Material online), then our results indicate that any one of the three observed β-chain substitutions could have occurred as the first step in the adaptive walk. However, as the initial substitution can significantly alter the sign and/or magnitude of the phenotypic effect of each subsequent mutation that occurs on the newly modified background, the selection coefficient (and, hence, fixation probability) of each new mutation will be historically contingent on which affinity-enhancing mutation happened to be the first one to fix. This role for contingency also holds in cases where the epistatically interacting sites are simultaneously polymorphic.

Conclusions

The functional effects of affinity-altering mutations in pika Hb were highly dependent on the sequential order in which they occurred. Two of the historical β-globin substitutions in *O. princeps* increased or decreased Hb–O_2 affinity depending on whether they occurred as the first step or the last step in the mutational pathway. Regardless of the temporal order in which the three β-chain substitutions actually occurred during the evolution of the increased Hb–O_2 affinity in *O. princeps*, our results revealed no evidence for ineluctable pleiotropic trade-offs that could constrain mutational pathways of Hb evolution. These results suggest that the accessibility of alternative mutational pathways may be more strongly constrained by sign epistasis for positively selected biochemical phenotypes than by antagonistic pleiotropy. The caveat is that this inference is only valid for the circumscribed region of sequence space that we examined, and for the particular biochemical properties that we investigated. In contrast to the deleterious pleiotropic effects documented for spontaneous affinity-altering mutations in human Hb (Bellelli et al. 2006; Storz and Moriyama 2008; Varnado et al. 2013), the mutations that have contributed to evolutionary changes in Hb–O_2 affinity in *O. princeps* produced fine-tuned changes in O_2-affinity with minimal pleiotropic effects. These findings are consistent with theory suggesting that function-altering mutations with minimal pleiotropic effects will tend to make disproportionate contributions to phenotypic evolution (Otto 2004; Streisfeld and Rausher 2011).

Materials and Methods

Specimen Collection

For the survey of *HBA* and *HBB* sequence variation and the functional analyses of native Hbs, we collected seven *O. princeps* near the summit of Mt. Evans, Clear Creek Co., Colorado (39°15′24″N, 106°10′54″W; 4,262 m above sea level [a.s.l.]) and a total of six *O. collaris* from Eagle Summit, Yukon-Koyukuk Co., Alaska (65°29′8″N, 145°24′0″W; 949 m a.s.l.) and Rainbow Ridge, Fairbanks North Star Co., Alaska (66°18′32″N, 145°40′21″W; 1,119 m a.s.l.). Specimens of *O. princeps* were collected under permit 10TR2058 from the Colorado Division of Wildlife, and were deposited as voucher specimens in the Harold W. Manter Laboratory collection of the University of Nebraska State Museum (HWML; catalog nos. NP1195, 1201–1202). Specimens of *O. collaris* were collected under permit 11-057 from the Alaska Department of Fish and Game and were deposited as voucher specimens in the University of Alaska Museum of the North (UAMN; UAM111535, 111549, 111591, 111675, 111698, and 111847). Pikas were euthanized in accordance with guidelines approved by the University of Nebraska Institutional Animal Care and Use Committee (IACUC no. 519). Blood was collected from each animal through cardiac puncture and red cell fractions were snap-frozen in liquid nitrogen. Liver tissue samples were also collected from each individual as a source of genomic DNA. Liver samples were immediately frozen in liquid nitrogen and stored at −80 °C prior to DNA extraction.

To conduct a broader survey of intraspecific DNA polymorphism in the *HBA* and *HBB* genes, we augmented our sample of wild-caught pikas with frozen tissue samples from additional specimens of *O. princeps* and *O. collaris* from the University of California Museum of Vertebrate Zoology (MVZ 202371) and UAMN (UAM 100795, 102429, 102435). To sequence orthologous *HBA* and *HBB* genes in other pika species, we obtained tissue samples from field-collected specimens of *O. daurica* ($n = 3$) from Khan Taishir Mountain, Mongolia (46°14′23″N, 96°21′30″E; 1,965 m a.s.l.) and *O. pallasi* ($n = 1$) from Jargalant Khairkhan Mountain, Mongolia (47°44′21″N, 92°27′24″E; 1,724 m a.s.l.). Voucher specimens were exported under permit G.12.15 and were deposited in the HWML collection (NK223524–223526, 223869). We obtained frozen tissue samples of *O. rufescens* (MVZ 191920) and *O. hyperborea* (UAM 84368), and we retrieved *O. curzoniae HBA* and *HBB* sequences from GenBank (EF429202 and DQ839484, respectively).

DNA Sequencing

For each pika specimen, genomic DNA was extracted from liver tissue using the DNeasy Blood and Tissue kit according to the manufacturer's protocol (Qiagen, Valencia, CA). We polymerase chain reaction (PCR)-amplified the *HBA* and *HBB* genes of each of the examined pika species using the Expand High Fidelity PCR system (Roche Applied Science, Indianapolis, IN). For the survey of polymorphism in each of the two focal species, we sequenced both alleles of the *HBA* and *HBB* genes (for each gene, $n = 16$ and 18 alleles for *O. princeps* and *O. collaris*, respectively). Thermal cycler conditions were as follows: An initial denaturing step for 2 min, followed by 35 cycles of 94 °C for 30 s, 55–57 °C for 30 s, 72 °C for 2 min, and final extension of 72 °C for 10 min. Primers for the PCR-amplification of the *HBA* and *HBB* genes are provided in supplementary table S3, Supplementary Material online. PCR products were purified and sequenced bidirectionally. All sequences were deposited in GenBank under the following accession numbers: KC757706–757708, KC757676–KC757683, KC757705, KC757674, KC757675, KC757684, KC757685, KC757646, KC757688, KC757689, KC757648–757653, KC757690, KC757654, KC757655, KC757691-757696, KC757656–757661, KC757697–757704, KC757662–757673, KC757686, KC757687, and KC757647.

Molecular Evolution Analyses

To make inferences about patterns of molecular evolution and to reconstruct ancestral sequences we estimated separate phylogenies for the *HBA* and *HBB* genes of pikas, using the rabbit orthologs as outgroup sequences. We aligned the nucleotide sequences based on their conceptually translated amino acid sequences using MAFFT (version 7.182, Katoh and Standley 2013) and we then performed phylogeny reconstructions using maximum likelihood as implemented in Treefinder, ver March 2011 (Jobb et al. 2004). We evaluated support for the nodes with 1,000 bootstrap pseudoreplicates. We used the "propose model" tool of Treefinder to select the best-fitting models of nucleotide substitution for each codon

position based on the Akaike information criterion with correction for small sample size. The estimated trees were used for all downstream analyses.

To reconstruct the HBB amino acid sequence of the *princeps/collaris* common ancestor, we used a maximum-likelihood approach (Yang et al. 1995) as implemented in PAML 4.8 (Yang 2007). To test for evidence of positive selection in pika *HBA* and *HBB* genes, we quantified variation in ω ($=d_N/d_S$, the ratio of the rate of nonsynonymous substitution per nonsynonymous site [d_N] to the rate of synonymous substitution per synonymous site [d_S] site) using a maximum-likelihood approach (Goldman and Yang 1994) implemented in the CODEML program, v. 4.8 (Yang 2007). In all cases, we used LRTs to compare nested sets of models (Yang 1998). We first compared models that allow ω to vary among codons in the alignments of *HBA* and *HBB* coding sequence (M0 vs. M3, M1a vs. M2a, M7 vs. M8). The latter two LRTs are tests of positive selection, as the alternative models (M2a and M8) allow a subset of sites to have $\omega > 1$, in contrast to the null models (M1a and M7) that only include site classes with $\omega < 1$. These analyses revealed statistically significant variation in ω among sites in the *HBB* alignment (supplementary table S2, Supplementary Material online), so we then implemented branch and branch-site analyses. The branch-site analyses permit inferences about changes in the selective regime in a subset of codons between foreground and background branches (Yang and Nielsen 2002; Yang et al. 2005; Yang and dos Reis 2011). In the alternative hypothesis (Model A), a fraction of sites in foreground branches are permitted to shift to a regime of positive selection (indicated by $\omega > 1$); under the null model, in contrast, sites are only permitted to shift between neutral evolution and purifying selection. We implemented three different branch models: 1) A single-ω model, where all branches in the tree had the same ω, which corresponds to M0 from the sites analyses; 2) a two-ω model, involving a joint estimate of ω for branches subtending the two high-altitude species (*O. curzionae* and *O. princeps*) and a separate estimate of ω for the remaining "background" branches; and 3) a three-ω model with separate ω estimates for *O. curzionae*, *O. princeps*, and all background branches. We then conducted branch-site analyses of *HBB* sequences that focused specifically on *O. princeps*. We compared two sets of models, one in which the branch subtending the set of *O. princeps* sequences was set as the foreground branch, and one in which the entire set of *O. princeps* sequences (*O. princeps* clade) was set as foreground. We used the Bayes Empirical Bayes approach to calculate the posterior probability that a given site belongs to the site class with $\omega > 1$ (i.e., that the substitution at the site in question was driven by positive selection in the foreground branch) (Yang et al. 2005).

Native Hb Purification

We used isoelectric focusing (PhastSystem, GE Healthcare Bio-Sciences, Piscataway, NJ) to characterize the Hb isoform composition of circulating red blood cells in both *O. princeps* and *O. collaris*. Native pika Hbs were purified by means of anion-exchange chromatography (HiTrap QHP, GE Healthcare, Piscataway, NJ), as described previously (Storz et al. 2012; Revsbech et al. 2013). The column was pre-equilibrated with 20 mM Tris (pH 8.4) and the sample was eluted using a linear gradient of 0–0.2 M NaCl. Samples were desalted by dialysis against 10 mM HEPES buffer (pH 7.4) and were concentrated using Millipore centrifugal filter units (30-kDa cutoff). Hb concentrations were determined from absorbance spectra using standard extinction coefficients at 577 and 540 nm.

Vector Construction and Site-Directed Mutagenesis

Nucleotide sequences of pika *HBA* and *HBB* genes were optimized with respect to *Escherichia coli* codon preferences, and were then synthesized by Eurofins (Huntsville, AL). Gene cassettes for the *HBA* and *HBB* genes and the *methionine aminopeptidase* (*MAP*) gene were tandemly cloned into the custom expression vector (pGM plasmid) described by Natarajan et al. (2011, 2013). In order to maximize efficiency in the posttranslational cleaving of N-terminal methionine residues from the nascent α- and β-chain polypeptides, an additional copy of the *MAP* gene was cloned into a coexpressed plasmid, pCO-MAP, with a kanamycin resistance gene. Site-directed mutagenesis was performed using the QuikChange II XL Site-Directed Mutagenesis kit from Stratagene (La Jolla, CA). Each engineered codon change in the globin cassette was verified by plasmid sequencing. Sequences for the mutagenic primers are provided in supplementary table S3, Supplementary Material online.

Expression and Purification of rHb

All rHb mutants were expressed in the JM109 (DE3) *E. coli* strain as described previously (Natarajan et al. 2011, 2013; Projecto-Garcia et al. 2013; Cheviron et al. 2014). Bacterial cells were subject to dual selection in an LB agar plate containing ampicillin and kanamycin, which ensures that transformed cells receive both the pGM and pCO-MAP plasmids. High-level expression of *MAP* enzyme proved critical for synthesizing fully functional rHbs. All pika rHb mutants were expressed in identical experimental conditions. Large-scale production was conducted in batches containing 1.5–2.0 l of TB medium. Cells were grown at 37 °C in an orbital shaker at 200 rpm until the absorbance reached an optical density of 0.6 at 600 nm. Expression of the *HBA*, *HBB*, and *MAP* genes was induced with 0.2 mM IPTG and the culture was supplemented with hemin (50 μg/ml) and glucose (20 g/l). The cells were then grown at 28 °C for 16 h in an orbital shaker at 200 rpm. The bacterial culture was saturated with CO for 15 min and the cells were harvested by centrifugation and stored at −80 °C.

As a preparative step for the protein purification, the cells were resuspended in lysis buffer (50 mM Tris, 1 mM ethylenediaminetetraacetic acid [EDTA], 0.5 mM DTT, pH 7.6) with lysozyme (1 mg/g wet cells) and were incubated in an ice bath for 30 min. The bacterial cells were sonicated, followed by addition of polyethyleneimine solution (0.5–1%) and centrifugation at 13,000 rpm (4 °C) for 45 min. The clarified

supernatant was then subjected to overnight dialysis in Tris buffer (20 mM Tris–HCl with 0.5 mM EDTA, pH 8.3). The rHbs were then purified by two-step ion-exchange chromatography. We used prepacked Q-Sepharose columns (HiTrap QHP, 5 ml, 17-1154-01; GE Healthcare) equilibrated with Tris-buffer (20 mM Tris–HCl with 0.5 mM EDTA, pH 8.3). The samples were passed through the column and the rHb solutions were eluted against a linear gradient of 0–0.5 M NaCl. The eluted samples were desalted by overnight dialysis with phosphate buffer (10 mM sodium phosphate buffer, 0.5 mM EDTA, pH 6.8). Each dialyzed rHb sample was then passed through an SP-Sepharose column (HiTrap SPHP, 1 ml, 17-1151-01; GE Healthcare) with an elution buffer (20 mM sodium phosphate buffer, 0.5 mM EDTA, pH 8.3). Samples were concentrated and desalted by overnight dialysis against 10 mM HEPES buffer (pH 7.4) and were stored at −80 °C prior to the measurement of O_2-equilibrium curves and autoxidation rates. The purity of each rHb preparation was confirmed by 20% sodium dodecyl sulfate-polyacrylamide gel electrophoresis and measures of the absorbance spectra of oxy, deoxy, and CO derivatives at 450–600 nm.

Experimental Measurements of Hb Function

Measures of Hb–O_2 affinity were conducted using a modified diffusion chamber where changes in absorbance were recorded in conjunction with stepwise changes in the O_2 tension of equilibration gases, as described previously (Weber 1992; Runck et al. 2010; Grispo et al. 2012; Storz et al. 2012; Revsbech et al. 2013). Measured O_2-equilibrium curves were based on 4–6 saturation steps. Values of P_{50} (partial pressure of O_2 [PO_2] at half-saturation) and the cooperativity coefficient, n_{50}, were calculated by using nonlinear regression to fit the O_2-saturation data to the Hill equation ($Y = PO_2^n / [P_{50}^n + PO_2^n]$, where Y is the fractional O_2 saturation and n is the cooperativity coefficient). O_2-binding equilibria of native and rHb solutions (0.3 mM heme) were measured at 37 °C in 0.1 M HEPES buffer, pH 7.4, in the absence (stripped) and presence of added allosteric effectors (0.1 M KCl, and/or DPG at 2.0-fold molar excess over tetrameric Hb). These are standard experimental conditions (Imai 1982; Mairbäurl and Weber 2012) that closely approximate intraerythrocytic effector concentrations in vivo: 100 mM Cl^- approximates the naturally occurring concentration inside mammalian red blood cells (where K^+ is the main counter ion, as opposed to Na^+ in the plasma) and a DPG/Hb tetramer ratio = 2.0 falls within the physiological range for most eutherian mammals (Bunn 1971; Duhm 1971; Mairbäurl and Weber 2012; Tufts et al. 2013). Hb–O_2 equilibria at physiological concentrations of Cl^- ions and DPG ensure that the in vitro measurements are relevant to in vivo conditions (Mairbäurl and Weber 2012). Possible discrepancies in the measured P_{50} values for native Hbs and rHb mutants could stem from the fact that the native Hb samples are characterized by some degree of structural heterogeneity due to heterozygosity at α- and/or β-globin sites, whereas rHbs have an invariant amino acid composition. For this reason, all inferences are based on comparisons between native Hbs of the two species (table 1), or comparisons among the rHb mutants (supplementary table S1, Supplementary Material online).

To characterize the pleiotropic effects of affinity-altering mutations, we measured four properties that can potentially trade-off with Hb–O_2 affinity: Structural mobility, cooperativity of O_2-binding, allosteric regulatory capacity (the sensitivity of Hb–O_2 affinity to the inhibitory effects of anionic effectors), and susceptibility to spontaneous heme oxidation (autoxidation rate; supplementary table S1, Supplementary Material online). Although there are numerous potential pleiotropic effects of amino acid mutations that could be measured, we chose to focus on four quantifiable properties that are of known importance and physiological relevance (Olson and Maillett 2005; Bonaventura et al. 2013; Varnado et al. 2013). To predict structural mobility of tetrameric Hb, we used the crystal structure of European hare Hb (*Lepus europaeus*; PDB ID, 3LQD) to build a structural model of pika Hb using SWISS-MODEL (Arnold et al. 2006); derivatives were modeled using MODELLER 9V11 (Sali and Blundell 1993). Molecular interactions were identified by PISA (Krissinel and Henrick 2007), and molecular graphics were generated using PyMol (Schrödinger, LLC). Conformational stress and ligand binding energy were computed using the Frustratometer (Jenik et al. 2012) and AutoDock (Morris et al. 2009) programs. As a measure of cooperativity, we used Hill's coefficient (n_{50}) in the presence of Cl^- and DPG. As a measure of allosteric regulatory capacity, we measured the difference in log-transformed P_{50} values for stripped Hb in the presence and absence of KCl and DPG. Following standard protocols for vertebrate Hbs (Jensen 2001), we measured autoxidation rates of purified rHbs at 10 μM concentration in 50 mM Tris buffer pH 7.4 at 37 °C using an Agilent 8453 UV-Visible Spectrophotometer (Agilent Technologies, Santa Clara, CA). Absorbance was recorded every hour at 560, 576, and 630 nm over a 14-h period. For each experiment, measurements of autoxidation rates were derived from the average of absorbance traces from the three wavelengths.

Supplementary Material

Supplementary tables S1–S3 are available at *Molecular Biology and Evolution* online (http://www.mbe.oxfordjournals.org/).

Acknowledgments

The authors thank L.E. Olson, A.M. Gunderson, S.L. Gardner, K. Roccaforte, Z.A. Cheviron, and A.M. Runck for assistance in the field, K. G. McCracken, L. E. Olson, and A. M. Gunderson for logistical support in Alaska, and H.C. Lanier for helpful discussions. They are also grateful to four anonymous reviewers for insightful comments on the manuscript. This research was funded by grants from the National Institute of Health (HL087216) to J.F.S.; the American Society of Mammalogists to D.M.T.; the School of Biological Sciences, University of Nebraska to D.M.T.; the Carlsberg Foundation (2013-01-0178) to A.F.; and the Faculty of Science and Technology, Aarhus University to A.F. and R.E.W.

References

Arnold K, Bordoli L, Kopp J, Schwede T. 2006. The SWISS-MODEL workspace: a web-based environment for protein structure homology modelling. *Bioinformatics* 22:195–201.

Baldwin J, Chothia C. 1979. Haemoglobin: the structural changes related to ligand binding and its allosteric mechanism. *J Mol Biol.* 129: 175–220.

Bellelli A, Brunori M, Miele AE, Panetta G, Vallone B. 2006. The allosteric properties of hemoglobin: insights from natural and site directed mutants. *Curr Protein Pept Sci.* 7:17–45.

Bettati S, Mozzarelli A, Perutz MF. 1983. Allosteric mechanism of hemoglobin: rupture of salt bridges raises oxygen affinity of the T-structure. *J Mol Biol.* 281:581–585.

Beutler E, Lang A, Lehmann H. 1974. Hemoglobin Duarte: ($\alpha_2\beta_2^{62(E6)Ala\rightarrow Pro}$): a new unstable hemoglobin with increased oxygen affinity. *Blood* 43:527–535.

Bloom JD, Labthavikul ST, Otey CR, Arnold FH. 2006. Protein stability promotes evolvability. *Proc Natl Acad Sci U S A.* 103:5869–5874.

Bonaventura C, Henkens R, Alayash AI, Banerjee S, Crumbliss AL. 2013. Molecular controls of the oxygenation and redox reactions of hemoglobin. *Antioxid Redox Signal.* 18:2298–2313.

Bridgham JT, Ortlund EA, Thornton JW. 2009. An epistatic ratchet constrains the direction of glucocorticoid receptor evolution. *Nature* 461:515–519.

Bunn HF. 1971. Differences in interaction of 2,3-diphosphoglycerate with certain mammalian hemoglobins. *Science* 172:1049–1050.

Carneiro M, Hartl DL. 2010. Adaptive landscapes and protein evolution. *Proc Natl Acad Sci U S A.* 107:1747–1751.

Ceccarelli M, Ruggerone P, Anedda R, Fais A, Era B, Sollaino MC, Corda M, Casu M. 2006. Structure-function relationship in a variant hemoglobin: a combined computational-experimental approach. *Biophys J.* 91:3529–3541.

Cheviron ZA, Natarajan C, Projecto-Garcia J, Eddy DK, Jones J, Carling MD, Witt CC, Moriyama H, Weber RE, Fago A, et al. 2014. Integrating evolutionary and functional tests of adaptive hypotheses: a case study of altitudinal differentiation in hemoglobin function in an Andean sparrow, *Zonotrichia capensis*. *Mol Biol Evol.* 31: 2948–2962.

da Silva J, Coetzer M, Nedellec R, Pastore C, Mosier DE. 2010. Fitness epistasis and constraints on adaptation in a human immunodeficiency virus type 1 protein region. *Genetics* 185:293–303.

de Visser JAGM, Krug J. 2014. Empirical fitness landscapes and the predictability of evolution. *Nat Rev Genet.* 15:480–490.

DePristo MA, Hartl DL, Weinreich DM. 2007. Mutational reversions during adaptive protein evolution. *Mol Biol Evol.* 24:1608–1610.

DePristo MA, Weinreich DM, Hartl DL. 2005. Missense meanderings in sequence space: a biophysical view of protein evolution. *Nat Rev Genet.* 6:678–687.

Draghi JA, Plotkin JB. 2013. Selection biases the prevalence and type of epistasis along adaptive trajectories. *Evolution* 67:3120–3131.

Duhm J. 1971. Effects of 2,3-diphosphoglycerate and other organic phosphate compounds on oxygen affinity and intracellular pH of human erythrocytes. *Pflugers Arch.* 326:341.

Dumoulin A, Manning LR, Jenkins WT, Winslow RM, Manning JM. 1997. Exchange of subunit interfaces between recombinant adult and fetal hemoglobins—evidence for a functional inter-relationship among regions of the tetramer. *J Biol Chem.* 272:31326–31332.

Dumoulin A, Padovan JC, Manning LR, Popowicz A, Winslow RM, Chait BT, Manning JM. 1998. The N-terminal sequence affects distant helix interactions in hemoglobin—implications for mutant proteins from studies on recombinant hemoglobin felix. *J Biol Chem.* 273: 35032–35038.

Erbajeva MA. 1994. Phylogeny and evolution of Ochotonidae with emphasis on Asian ochotonids. In: Tomida Y, Li CK, Setoguchi T, editors. Rodent and lagomorph families of Asian origins and diversification. Proceedings of Workshop WC-2, 29th International Geological Congress, Kyoto, Japan. Tokyo: National Science Museum Monographs. p. 1–13.

Galbreath KE, Hafner DJ, Zamudio KR. 2009. When cold is better: climate-driven elevation shifts yield complex patterns of diversification and demography in an alpine specialist (American pika, *Ochotona princeps*). *Evolution* 63:2848–2863.

Galbreath KE, Hafner DJ, Zamudio KR, Agnew K. 2010. Isolation and introgression in the Intermountain West: contrasting gene genealogies reveal the complex biogeographic history of the American pika (*Ochotona princeps*). *J Biogeogr.* 37:344–362.

Goldman N, Yang ZH. 1994. Codon-based model of nucleotide substitution for protein-coding DNA sequences. *Mol Biol Evol.* 11:725–736.

Gong LI, Bloom JD. 2014. Epistatically interacting substitutions are enriched during adaptive protein evolution. *PLoS Genet.* 10:e1004328.

Grispo MT, Natarajan C, Projecto-Garcia J, Moriyama H, Weber RE, Storz JF. 2012. Gene duplication and the evolution of hemoglobin isoform differentiation in birds. *J Biol Chem.* 287:12.

Hafner DJ. 1993. North American pika (*Ochotona princeps*) as a Late Quaternary biogeographic indicator species. *Quat Res.* 39:373–380.

Hafner DJ. 1994. Pikas and permafrost: post-Wisconsin historical zoogeography of *Ochotona* in the Southern Rocky Mountains, USA. *Arct Alp Res.* 26:375–382.

Harms MJ, Thornton JW. 2014. Historical contingency and its biophysical basis in glucocorticoid receptor evolution. *Nature* 512: 203–207.

Imai K. 1982. Allosteric effects in haemoglobin. Cambridge: Cambridge University Press.

Jenik M, Gonzalo Parra R, Radusky LG, Turjanski A, Wolynes PG, Ferreiro DU. 2012. Protein frustratometer: a tool to localize energetic frustration in protein molecules. *Nucleic Acids Res.* 40:W348–W351.

Jensen FB. 2001. Comparative analysis of autoxidation of haemoglobin. *J Exp Biol.* 204:2029–2033.

Jobb G, von Haeseler A, Strimmer K. 2004. TREEFINDER: a powerful graphical analysis environment for molecular phylogenetics. *BMC Evol Biol.* 4:18.

Katoh K, Standley DM. 2013. MAFFT multiple sequence alignment software version 7: improvements in performance and usability. *Mol Biol Evol.* 30:772–780.

Krissinel E, Henrick K. 2007. Inference of macromolecular assemblies from crystalline state. *J Mol Biol.* 372:774–797.

Kryazhimskiy S, Dushoff J, Bazykin GA, Plotkin JB. 2011. Prevalence of epistasis in the evolution of influenza A surface proteins. *PLoS Genet.* 7:e1001301.

Kryazhimskiy S, Rice DP, Jerison ER, Desai MM. 2014. Global epistasis makes adaptation predictable despite sequence-level stochasticity. *Science* 344:1519–1522.

Kvitek DJ, Sherlock G. 2011. Reciprocal sign epistasis between frequently experimentally evolved adaptive mutations causes a rugged fitness landscape. *PLoS Genet.* 7:e1002056.

Lanier HC, Olson LE. 2009. Inferring divergence times within pikas (*Ochotona* spp.) using mtDNA and relaxed molecular dating techniques. *Mol Phylogenet Evol.* 53:1–12.

Lanier HC, Olson LE. 2013. Deep barriers, shallow divergences: reduced phylogeographical structure in the collared pika (Mammalia: Lagomorpha: *Ochotona collaris*). *J Biogeogr.* 40:466–478.

Lopez-Llano J, Campos LA, Sancho J. 2006. α-helix stabilization by alanine relative to glycine: roles of polar and apolar solvent exposures and of backbone entropy. *Proteins* 64:769–778.

Lozovsky ER, Chookajorn T, Brown KM, Imwong M, Shaw PJ, Kamchonwongpaisan S, Neafsey DE, Weinreich DM, Hartl DL. 2009. Stepwise acquisition of pyrimethamine resistance in the malaria parasite. *Proc Natl Acad Sci U S A.* 106:12025–12030.

Mairbäurl H. 1994. Red blood cell function in hypoxia at altitude and exercise. *Int J Sports Med.* 15:51–63.

Mairbäurl H, Weber RE. 2012. Oxygen transport by hemoglobin. *Compr Physiol.* 2:1463–1489.

Mead JI. 1987. Quaternary records of the pika, *Ochotona*, in North America. *Boreas* 16:165–171.

Morris GM, Huey RB, Lindstrom W, Sanner MF, Belew RK, Goodsell DS, Olson AJ. 2009. Autodock4 and AutoDockTools4: automated docking with selective receptor flexibility. *J Comput Chem.* 16:2785–2791.

Natarajan C, Inoguchi N, Weber RE, Fago A, Moriyama H, Storz JF. 2013. Epistasis among adaptive mutations in deer mouse hemoglobin. *Science* 340:1324–1327.
Natarajan C, Jiang X, Fago A, Weber RE, Moriyama H, Storz JF. 2011. Expression and purification of recombinant hemoglobin in *Escherichia coli*. *PLoS One* 6:e20176.
Olson JS, Maillett DH. 2005. Designing recombinant hemoglobin for use as a blood substitute. In: Winslow RM, editor. Blood substitutes. San Diego (CA): Academic Press. p. 354–374.
Ortlund EA, Bridgham JT, Redinbo MR, Thornton JW. 2007. Crystal structure of an ancient protein: evolution by conformational epistasis. *Science* 317:1544–1548.
Ostman B, Hintze A, Adami C. 2012. Impact of epistasis and pleiotropy on evolutionary adaptation. *Proc R Soc Lond B Biol Sci.* 279:247–256.
Otto SP. 2004. Two steps forward, one step back: the pleiotropic effects of favoured alleles. *Proc R Soc Lond B Biol Sci.* 271:705–714.
Perutz MF. 1972. Nature of haem-haem interaction. *Nature* 237: 495–499.
Perutz MF. 1989. Mechanisms of cooperative and allosteric regulation in proteins. *Q Rev Biophys.* 22:139–237.
Poelwijk FJ, Kiviet DJ, Weinreich DM, Tans SJ. 2007. Empirical fitness landscapes reveal accessible evolutionary paths. *Nature* 445:383–386.
Projecto-Garcia J, Natarajan C, Moriyama H, Weber RE, Fago A, Cheviron ZA, Dudley R, McGuire JA, Witt CC, Storz JF. 2013. Repeated elevational transitions in hemoglobin function during the evolution of Andean hummingbirds. *Proc Natl Acad Sci U S A.* 110:20669–20674.
Revsbech IG, Tufts DM, Projecto-Garcia J, Moriyama H, Weber RE, Storz JF, Fago A. 2013. Hemoglobin function and allosteric regulation in semi-fossorial rodents (family Sciuridae) with different altitudinal ranges. *J Exp Biol.* 216:4264–4271.
Rokyta DR, Joyce P, Caudle SB, Miller C, Beisel CJ, Wichman HA. 2011. Epistasis between beneficial mutations and the phenotype-to-fitness map for a ssDNA virus. *PLoS Genet.* 7:e1002075.
Runck AM, Weber RE, Fago A, Storz JF. 2010. Evolutionary and functional properties of a two-locus b-globin polymorphism in Indian house mice. *Genetics* 184:1121–1131.
Sali A, Blundell TL. 1993. Comparative protein modeling by satisfaction of spatial restraints. *J Mol Biol.* 234:779–815.
Salverda MLM, Dellus E, Gorter FA, Debets AJM, van der Oost J, Hoekstra RF, Tawfik DS, de Visser JAGM. 2011. Initial mutations direct alternative pathways of protein evolution. *PLoS Genet.* 7: e1001321.
Smith AT, Weston ML. 1990. Ochotona princeps. *Mamm Species.* 352: 1–8.
Storz JF. 2007. Hemoglobin function and physiological adaptation to hypoxia in high-altitude mammals. *J Mammal.* 88:24–31.
Storz JF, Moriyama H. 2008. Mechanisms of hemoglobin adaptation to high altitude hypoxia. *High Alt Med Biol.* 9:148–157.
Storz JF, Runck AM, Moriyama H, Weber RE, Fago A. 2010. Genetic differences in hemoglobin function between highland and lowland deer mice. *J Exp Biol.* 213:2565–2574.
Storz JF, Runck AM, Sabatino SJ, Kelly JK, Ferrand N, Moriyama H, Weber RE, Fago A. 2009. Evolutionary and functional insights into the mechanism underlying high-altitude adaptation of deer mouse hemoglobin. *Proc Natl Acad Sci U S A.* 106:14450–14455.
Storz JF, Scott GR, Cheviron ZA. 2010. Phenotypic plasticity and genetic adaptation to high-altitude hypoxia in vertebrates. *J Exp Biol.* 213: 4125–4136.
Storz JF, Weber RE, Fago A. 2012. Oxygenation properties and oxidation rates of mouse hemoglobins that differ in reactive cysteine content. *Comp Biochem Physiol A Mol Integr Physiol.* 161:265–270.
Streisfeld MA, Rausher MD. 2011. Population genetics, pleiotropy, and the preferential fixation of mutations during adaptive evolution. *Evolution* 65:629–642.
Taverna DM, Goldstein RA. 2002. Why are proteins marginally stable? *Proteins* 46:105–109.
Tokuriki N, Stricher F, Serrano L, Tawfik DS. 2008. How protein stability and new functions trade off. *PLoS Comput Biol.* 4:e1000002.
Tokuriki N, Tawfik DS. 2009. Stability effects of mutations and protein evolvability. *Curr Opin Struct Biol.* 19:596–604.
Tufts DM, Revsbech IG, Cheviron ZA, Weber RE, Fago A, Storz JF. 2013. Phenotypic plasticity in blood-oxygen transport in highland and lowland deer mice. *J Exp Biol.* 216:1167–1173.
Turek Z, Kreuzer F. 1976. Effect of a shift of the oxygen dissociation curve on myocardial oxygenation at hypoxia. *Adv Exp Med Biol.* 75: 657–662.
Turek Z, Kreuzer F, Ringnalda BEM. 1978. Blood gases at several levels of oxygenation in rats with a left-shifted blood oxygen dissociation curve. *Pflügers Arch.* 376:7–13.
Turek Z, Kreuzer F, Turek-Maischeider M, Ringnalda BEM. 1978. Blood oxygen content, cardiac output, and flow to organs at several levels of oxygenation in rats with a left-shifted blood oxygen dissociation curve. *Pflügers Arch.* 376:201–207.
Varnado CL, Mollan TL, Birukou I, Smith BJZ, Henderson DP, Olson JS. 2013. Development of recombinant hemoglobin-based oxygen carriers. *Antioxid Redox Signal.* 18:2314–2328.
Wang XJ, Minasov G, Shoichet BK. 2002. Evolution of an antibiotic resistance enzyme constrained by stability and activity trade-offs. *J Mol Biol.* 320:85–95.
Weber RE. 1992. Use of ionic and zwitterionic (tris bistris and HEPES) buffers in studies on hemoglobin function. *J Appl Physiol.* 72: 1611–1615.
Weber RE. 2007. High-altitude adaptations in vertebrate hemoglobins. *Respir Physiol Neurobiol.* 158:132–142.
Weinreich DM, Delaney NF, DePristo MA, Hartl DL. 2006. Darwinian evolution can follow only very few mutational paths to fitter proteins. *Science* 312:111–114.
Weinreich DM, Knies JL. 2013. Fisher's geometric model of adaptation meets the functional synthesis: data on pairwise epistasis for fitness yields insights into the shape and size of phenotype space. *Evolution* 67:2957–2972.
Weinreich DM, Watson RA, Chao L. 2005. Sign epistasis and genetic constraint on evolutionary trajectories. *Evolution* 59: 1165–1174.
Yang Z. 2007. PAML 4: Phylogenetic analysis by maximum likelihood. *Mol Biol Evol.* 24:1586–1591.
Yang Z, dos Reis M. 2011. Statistical properties of the branch-site test of positive selection. *Mol Biol Evol.* 28:1217–1228.
Yang ZH. 1998. Likelihood ratio tests for detecting positive selection and application to primate lysozyme evolution. *Mol Biol Evol.* 15: 568–573.
Yang ZH, Kumar S, Nei M. 1995. A new method of inference of ancestral nucleotide and amino-acid sequences. *Genetics* 141:1641–1650.
Yang ZH, Nielsen R. 2002. Codon-substitution models for detecting molecular adaptation at individual sites along specific lineages. *Mol Biol Evol.* 19:908–917.
Yang ZH, Wong WSW, Nielsen R. 2005. Bayes empirical Bayes inference of amino acid sites under positive selection. *Mol Biol Evol.* 22: 1107–1118.
Zhang JZ, Nielsen R, Yang ZH. 2005. Evaluation of an improved branch-site likelihood method for detecting positive selection at the molecular level. *Mol Biol Evol.* 22:2472–2479.

Table S1. Oxygenation properties, anion sensitivities, autoxidation rates, and predicted structural mobilities of purified pika rHbs. The eight rHb mutants represent a combinatorially complete set of β5-β62-β126 genotypes, including Anc1 (GAA), the derived, triple-mutant genotype of *O. princeps* (ATV), and each of six possible single- and double-mutant intermediates that connect them (see Fig. 4*B*). O_2-affinities (P_{50}) and cooperativity coefficients (n_{50}) (± SEM) were calculated from O_2-equilibrium curves measured at 0.3 mM heme in 0.1 M HEPES buffer at pH 7.4, 37° C, in the absence (stripped) and presence of added KCl (0.1 M) and/or DPG (DPG/Hb tetramer ratio, 2.0), as indicated. It was not possible to measure O_2-equilibrium curves for stripped samples of the AAA and GTA single-mutant genotypes due to rapid rates of heme oxidation during the course of the measurements. Sensivities to Cl^- ions and DPG were measured as $\Delta\log\text{-}P_{50([KCl+DPG]-[DPG])}$ and $\Delta\log\text{-}P_{50([KCl+DPG]-[KCl])}$, respectively. Measures of structural mobility are reported in arbitrary units (A.U.); the higher the value, the lower the predicted energetic frustration. See *Materials and Methods* for details.

	GAA	AAA	GTA	GAV	ATA	GTV	AAV	ATV
P_{50} (torr)								
stripped	5.25 ± 0.03	--	--	5.86 ± 0.35	4.36 ± 0.12	4.70 ± 0.19	3.92 ± 0.04	4.07 ± 0.01
+KCl	10.84 ± 0.25	9.77 ± 0.23	7.94 ± 0.12	8.62 ± 0.09	10.21 ± 0.33	8.63 ± 0.10	7.03 ± 0.06	8.13 ± 0.13
+DPG	11.02 ± 0.10	7.59 ± 0.20	6.61 ± 0.28	7.03 ± 0.03	8.09 ± 0.16	6.57 ± 0.02	6.67 ± 0.12	8.00 ± 0.05
+KCl+DPG	11.40 ± 0.14	9.81 ± 0.37	8.00 ± 0.37	7.72 ± 0.05	9.46 ± 0.12	7.83 ± 0.07	7.60 ± 0.14	8.92 ± 0.09
Cl^- sensitivity ($\Delta\log\text{-}P_{50}$)	0.015	0.111	0.072	0.041	0.066	0.059	0.078	0.047
DPG sensitivity ($\Delta\log\text{-}P_{50}$)	0.022	-0.002	0.004	-0.047	-0.026	0.038	-0.039	0.040
n_{50}								
stripped	2.27 ± 0.03	--	--	1.15 ± 0.09	1.82 ± 0.10	2.12 ± 0.18	2.13 ± 0.05	2.22 ± 0.01
+KCl	2.36 ± 0.11	1.66 ± 0.07	2.06 ± 0.15	2.13 ± 0.06	1.98 ± 0.13	2.09 ± 0.09	2.20 ± 0.05	2.26 ± 0.08
+DPG	2.38 ± 0.05	2.79 ± 0.28	4.59 ± 0.76	2.88 ± 0.05	2.61 ± 0.16	2.75 ± 0.03	2.36 ± 0.11	2.30 ± 0.03
+KCl+DPG	2.46 ± 0.07	2.54 ± 0.33	2.17 ± 0.29	2.57 ± 0.06	2.79 ± 0.13	2.43 ± 0.05	2.37 ± 0.12	2.34 ± 0.05
Autoxidation rate (s^{-1})	1.61×10^{-6}	5.66×10^{-5}	7.27×10^{-5}	3.88×10^{-5}	2.94×10^{-5}	-1.09×10^{-4}	3.96×10^{-5}	8.37×10^{-6}
Structural mobility (A.U.)	2.71	2.94	2.95	3.60	3.48	2.94	3.87	4.03

Table S2. Maximum-likelihood analysis of the ratio of nonsynonymous-to-synonymous substitution rates, ω (=d_N/d_S), in the *HBA* and *HBB* genes of pikas. Branch and branch-site analyses were only implemented for the *HBB* alignment, as the analysis of variation among sites in the *HBA* alignment did not detect statistically significant evidence of positive selection.

Model	**ln*L***	**No. parameters**	**Parameter estimates**	**Test**
HBA site-models				
M0	-1171.6	50	$\omega_0 = 0.22$	
M1a	-1169.6	51	$\omega_0 = 0.15$ ($p_0 = 0.86$) $\omega_1 = 1.00$	
M2	-1169.6	53	$\omega_0 = 0.15$ ($p_0 = 0.86$) $\omega_1 = 1.00$ ($p_1 = 0.08$) $\omega_2 = 1.00$	M2 vs M1 Not significant
M3	-1168.1	54	$\omega_0 = 0.00$ ($p_0 = 0.41$) $\omega_1 = 0.40$ ($p_1 = 0.39$) $\omega_2 = 0.40$	M3 vs M0 Not significant
M7	-1168.4	51	$p = 0.60$, $q = 1.87$	
M8	-1168.4	53	$p_0 = 0.99$; $p = 0.60$, $q = 1.87$ ($p_1 = 0.00001$) $\omega = 1.00$	M8 vs M7 Not significant
HBB site-models				
M0	-1547.9	64	$\omega_0 = 0.62$	
M1a	-1519.7	65	$\omega_0 = 0.02$ ($p_0 = 0.55$) $\omega_1 = 1.00$	
M2	-1512.3	67	$\omega_0 = 0.03$ ($p_0 = 0.55$) $\omega_1 = 1.00$ ($p_1 = 0.35$) $\omega_2 = 3.53$	M2 vs M1 $P < 0.001$
M3	-1512.3	68	$\omega_0 = 0.00$ ($p_0 = 0.48$) $\omega_1 = 0.80$ ($p_1 = 0.40$) $\omega_2 = 3.31$	M3 vs M0 $P < 0.001$
M7	-1519.9	65	$p = 0.02$, $q = 0.02$	
M8	-1512.5	67	$p_0 = 0.89$; $p = 0.08$, $q = 0.12$ ($p_1 = 0.11$) $\omega = 3.44$	M8 vs M7 $P < 0.001$
HBB branch-models				

Model	ln*L*	No. parameters	Parameter estimates					Test
1-ω	-1547.9	64	ω_0 = 0.62					
2-ω	-1547.9	65	$\omega_{background}$ = 0.64 $\omega_{curzionae+princeps}$ = 0.55					2-ω vs 1-ω Not significant
3-ω	-1546.6	66	$\omega_{background}$ = 0.64 $\omega_{princeps}$ = 1.07 $\omega_{curzionae}$ = 0.30					3-ω vs *2*-ω Not significant
HBB branch-site models								
O. princeps ancestral branch as foreground								
Model A null	-1519.5	66	Site class Proportion $\omega_{background}$ $\omega_{foreground}$	0 0.55 0.02 0.02	1 0.45 1.00 1.00	2a 0.00 0.02 1.00	2b 0.00 1.00 1.00	
Model A	-1519.7	67	Site class Proportion $\omega_{background}$ $\omega_{foreground}$	0 0.55 0.02 0.02	1 0.45 1.00 1.00	2a 0.00 0.02 1.00	2b 0.00 1.00 1.00	Model A vs A null Not significant
O. princeps clade as foreground								
Model A null	-1519.2	66	Site class Proportion $\omega_{background}$ $\omega_{foreground}$	0 0.47 0.01 0.01	1 0.36 1.00 1.00	2a 0.10 0.01 1.00	2b 0.08 1.00 1.00	
Model A[a]	-1516.4	67	Site class Proportion $\omega_{background}$ $\omega_{foreground}$	0 0.53 0.01 0.01	1 0.41 1.00 1.00	2a 0.03 0.01 16.70	2b 0.03 1.00 16.70	Model A vs A null $P < 0.025$

[a]Bayes empirical Bayes analysis implicated sites β62 and β126 as members of the positively selected site class (ω>1) with posterior probabilities of *P*=0.953 and 0.764, respectively.

Table S3. Sequences of primers used for PCR amplification and site-directed mutagenesis of pika *HBA* and *HBB* genes.

Gene	Primer name	Sequences (5'-3')
	Whole-gene amplification	
HBA	HBA-F	CAGCACCAGCCAATGACCGA
	HBA-R	ACAGGCTGCCACTCAGACTT
HBB	HBB-F	TGTCATCAGTCAGCCTCACC
	HBB-R	GGATTCGCACACAGCTCATA
Sites	**Site-Directed Mutagenesis**	
β5	OPB_G5A_SE	GGTGCATCTGAGCGCCGAAGAAAAAGCGG
	OPB_G5A_AS	CCGCTTTTTCTTCGGCGCTCAGATGCACC
β58	OPAB_P58A_SE	CGGTGATGGGCAACGCGAAAGTGAAAGCG
	OPAB_P58A_AS	CGCTTTCACTTTCGCGTTGCCCATCACCG
β62	OPB_A62T_SE	TGATGGGCAACGCGAAAGTGAAAACGCATG GCAAAA
	OPB_A62T_AS	TTTTGCCATGCGTTTTCACTTTCGCGTTGCCC ATCA
β123 &126	OPB_S123T_A126V_SE	GGCGGCGAATTTACCCCGCAGGTGCAGGCG
	OPB_S123T_A126V_AS	CGCCTGCACCTGCGGGGTAAATTCGCCGCC
β123	ANB_S123T_SE	TCTGGGCGGCGAATTTACCCCGCAGGC
	ANB_S123T_AS	GCCTGCGGGGTAAATTCGCCGCCCAGA